Cosmic acceleration, inflation, dark matter, and dark 'energy' in one neat package

Homer G. Ellis
*Department of Mathematics, University of Colorado at Boulder, Boulder, Colorado 80309**
(Dated: April 15, 2007)

In creating his gravitational field equations Einstein unjustifiedly assumed that inertial mass, and its energy equivalent, is a source of gravity. Denying this assumption allows modifying the field equations to a form in which a positive cosmological constant appears as a uniform density of gravitationally repulsive matter. Field equations with both positive and negative active gravitational mass densities incorporated along with a scalar field coupled to geometry with nostandard polarity yield cosmological solutions that exhibit acceleration, inflation, coasting, and a 'big bounce' instead of a 'big bang'. The repulsive matter is identified as the back sides of the 'drainholes' (called by some 'traversable wormholes') introduced by the author in 1973 as solutions of those same field equations. Drainholes are topological tunnels in space which gravitationally attract on their front, entrance sides and repel more strongly on their back, exit sides. The front sides serve as the unseen particles of 'dark matter' needed to hold together the large scale structures seen in the universe, the back sides, as the misnamed 'dark energy' driving the accelerating expansion of the universe. Formation of cosmic voids, walls, filaments, and nodes are attributed to separation of the back sides of the drainholes from the front, driven by their mutual attractive–repulsive interactions. One can assert that all of these cosmological entities have been found wrapped in one neat package, namely, the field equations and the variational principle from which they are derived.

PACS numbers: PACS numbers: 98.80.Jk, 98.80.Cq, 95.35.+d, 95.36.+x

I. EINSTEIN'S UNJUSTIFIED ASSUMPTION

Albert Einstein, in his 1916 paper Die Grundlage der allgemeinen Relativitätstheorie [1] that gave a thorough presentation of the theory of gravity he had worked out over the preceding decade, made an assumption that does not hold up well under close scrutiny. Stripped down to its barest form the assumption is that inertial mass, and by extension energy *via* $E = mc^2$, is a source of gravity and must therefore be coupled to the gravitational potential in the field equations of the general theory of relativity. The train of thought that brought him to this conclusion is described in §16, where he sought to extend his field equations for the vacuum, $\boldsymbol{R}_{\alpha\beta} - \frac{1}{2}\boldsymbol{R}g_{\alpha\beta} = 0$ as currently formulated, to include the contribution of a continuous distribution of gravitating matter of density μ, in analogy to the extension of the Laplace equation $\nabla^2\phi = 0$ for the newtonian gravitational potential ϕ to the Poisson equation $\nabla^2\phi = 4\pi\kappa\mu$, where κ is Newton's gravitational constant. Einstein referred to μ as the "density of matter", without specifying what was meant by 'matter' or its 'density'. Invoking the special theory's identification of "inert mass" with "energy, which finds its complete mathematical expression in ... the energy-tensor", he concluded that "we must introduce a corresponding energy-tensor of matter $\mathrm{T}^{\alpha}_{\sigma}$". Further describing this energy-tensor as "corresponding to the density μ in Poisson's equation", he arrived at the extended field equations $\boldsymbol{R}_{\alpha\beta} - \frac{1}{2}\boldsymbol{R}g_{\alpha\beta} = \frac{8\pi\kappa}{c^2}T_{\alpha\beta}$, in which, for a "frictionless adiabatic fluid" of "density" μ, pressure p (a form of kinetic energy), and proper 4-velocity distribution u^{α}, he took $T^{\alpha\beta}$ to be $\mu u^{\alpha}u^{\beta} + (p/c^2)(u^{\alpha}u^{\beta} - g^{\alpha\beta})$.

Clearly, Einstein's procedure fails to distinguish between the 'active gravitational mass' of matter, which measures how much gravity it produces and is the sole contributor to the "density of matter" in Poisson's equation, and the "inert mass" of matter, which measures how much it accelerates in response to forces applied to it, in concept an effect entirely different from the production of gravity. These two conceptually different masses, along with yet a third, all occur in Newton's gravitational equation

$$m_{\mathrm{i}}a_{\mathrm{B}} = F_{\mathrm{AB}} = -\kappa\frac{m_{\mathrm{p}}M_{\mathrm{a}}}{r^2}\,, \tag{1}$$

in which M_{a} is the *active* gravitational mass of a gravitating body A, m_{i} is the *inertial* ("inert") mass of a body B being acted upon by the gravity of A, and m_{p} is the *passive* gravitational mass of B, a measure of the strength of B's 'sensing' of the gravitational field around A. That in suitable units $m_{\mathrm{i}} = m_{\mathrm{p}}$ for all bodies is another way of saying that all bodies respond with the same accelerations to the same gravitational fields, that, in consequence, the notion of a 'gravitational force' is irrelevant, but the notion of a 'gravitational field' is not. Simple thought experiments of Galileo (large stone and smaller stone tied together) [2] and Einstein (body suspended by rope in elevator) [3] make it clear that bodies do all respond alike — an observation now treated as a principle, the (weak) 'principle of equivalence', experimentally, if somewhat redundantly, well confirmed. That this passive-inertial mass has any relation to active gravitational mass is not apparent in Eq. (1), where M_{a} represents a property of A, not of B. But Newton's equation

*URL: http://euclid.colorado.edu/~ellis; Electronic address: ellis@euclid.colorado.edu

for the gravitational action of B on A reads

$$M_{\rm i}a_{\rm A} = F_{\rm BA} = -\kappa\frac{M_{\rm p}m_{\rm a}}{r^2}\,. \qquad (2)$$

Application of Newton's law of action and reaction allows the inference that $F_{\rm AB}$ and $F_{\rm BA}$ have the same magnitude, from which follows that $m_{\rm a}/m_{\rm p} = M_{\rm a}/M_{\rm p}$, hence that the ratio of active gravitational mass to passive gravitational mass, thus to inertial mass, is the same for all bodies. It would seem likely that Einstein relied, either consciously or unconsciously, on this consequence of Newton's laws when he assumed that "inert mass" should contribute to the "density of matter" as a source of gravity in the field equations.

Newton's law of action and reaction is applicable to the bodies A and B only under the condition that gravity acts at a distance instantaneously, that is, at infinite propagation speed, whereas the general theory of relativity that Einstein was expounding is a field theory in which gravitational effects propagate at finite speed. Within his own theory of gravity there is, therefore, no obvious justification for Einstein's assumption that inertial mass (and therefore energy) is equivalent to active gravitational mass. This, however, is not to say that there is no relation at all between the two kinds of mass. There is, for example, the seemingly universal coincidence that wherever there is matter made of atoms there are to be found both inertial mass and active gravitational mass. Indeed, the fact that Newton's theory is a close first approximation to Einstein's would argue for some proportionality between $m_{\rm a}$ and $m_{\rm p}$ for such matter in bulk — not, however, for each individual constituent of such matter. A 1986 analysis of lunar data concluded that the ratio of $m_{\rm a}$ to $m_{\rm p}$ for aluminum differs from that of iron by less than 4×10^{-12} [4]. An earlier, Cavendish balance experiment had put a limit of 5×10^{-5} on the difference of these ratios for bromine and fluorine [5]. But these results are only for matter in bulk, that is, matter made of atoms and molecules. It is entirely possible that electrons, for example, do not gravitate at all, for no one has ever established by direct observation that they do, nor is it likely that anyone will. There is in the literature an argument that purports to show that if the ratio $m_{\rm a}/m_{\rm p}$ is the same for two species of bulk matter, then electrons must be generators of gravity [6], but that argument can be seen on careful examination to rest on an unrecognized, hidden assumption, namely that, in simplest form, the gravitational field of a hydrogen atom at a distance could be distinguished from that of a neutron at the same distance — another assumption no one has tested or is likely to test, by direct observation.

Einstein's assumption that energy and inertial mass are sources of gravity has survived to the present virtually unchallenged. It has generated a number of consequences that have directed much of the subsequent research in gravitation theory — indeed, misdirected it if his assumption is wrong. Among them are the following:

- The impossibility, according to Penrose–Hawking singularity theorems, of avoiding singularities in the geometry of space-time without invoking 'negative energy', which is really just energy coupled to gravity with polarity opposite to that of the coupling of matter to gravity.
- The presumption that the extra, fifth dimension in Kaluza–Klein theory must be a spatial dimension rather than a dimension of another type.
- The belief that all the extra dimensions in higher-dimensional theories must be spatial, causing the expenditure of much effort in attempting to explain why they are not apparent to our senses in the way that the familiar three spatial dimensions are.

Denying Einstein's assumption relieves one of the burden of these troublesome conclusions and opens the door to other, more realistic ones.

II. NEW FIELD EQUATIONS

If Einsteins's assumption is to be disallowed, then his source tensor for a continuous distribution of gravitating matter, $T^{\alpha\beta} = \mu u^\alpha u^\beta + (p/c^2)(u^\alpha u^\beta - g^{\alpha\beta})$, must be modified. One might think to simply drop the second term and take $T^{\alpha\beta} = \mu u^\alpha u^\beta$, the energy-momentum tensor of the matter. This would be inconsistent, for the μ in that tensor is the density of inertial-passive mass, which we are now not assuming to be the same as active gravitational mass. What to do instead?

At the same time that Einstein was creating his field equations, Hilbert was deriving the field equations for empty space from the variational principle $\delta\int \boldsymbol{R}\,|g|^{\frac12}d^4x = 0$ [7]. This is the most straightforward extension to the general relativity setting of the variational principle $\delta\int|\nabla\phi|^2\,d^3x = 0$, whose Euler–Lagrange equation is equivalent to the Laplace equation $\nabla^2\phi = 0$ for the newtonian potential ϕ. Modifying it to $\delta\int(|\nabla\phi|^2 + 8\pi\kappa\mu\phi)\,d^3x = 0$ generates the Poisson equation $\nabla^2\phi = 4\pi\kappa\mu$. The most straightforward extension of this principle to general relativity is

$$\delta\int(\boldsymbol{R} - \tfrac{8\pi\kappa}{c^2}\mu)\,|g|^{\frac12}d^4x = 0, \qquad (3)$$

for which the Euler–Lagrange equations are equivalent to

$$\boldsymbol{R}_{\alpha\beta} - \tfrac12\boldsymbol{R}\,g_{\alpha\beta} = -\tfrac{4\pi\kappa}{c^2}\mu g_{\alpha\beta}, \qquad (4)$$

which makes $T_{\alpha\beta} = -\frac12\mu g_{\alpha\beta}$, with μ now the *active* gravitational mass density, as it should be. Equivalent to this equation is $\boldsymbol{R}_{\alpha\beta} = \frac{4\pi\kappa}{c^2}\mu g_{\alpha\beta}$, the 00 component of which reduces in the slowly varying, weak field approximation precisely to the Poisson equation. The vanishing of the divergence of the Einstein tensor field on the lefthand side of Eq. (4) entails that $0 = T_\alpha{}^\beta{}_{:\beta} = -\frac12(\mu_{.\beta}g_\alpha{}^\beta + \mu g_\alpha{}^\beta{}_{:\beta}) = -\frac12\mu_{.\alpha}$, hence that μ is constant. This would seem to be a comedown from the

equations of motion of the matter distribution implied by the vanishing of the divergence of Einstein's $T^{\alpha\beta}$, but those equations are unrealistic in that they have the density of active mass playing the role that properly belongs to the density of inertial mass as the coefficient of the 4-acceleration of the matter. The implied constancy of μ will be seen not to be a harmful defect of the revised field equations.

To include contributions of other suspected determinants of the geometry of space-time, such as scalar fields and electromagnetic fields, one can in the usual way add terms to the action integrand of Eq. (3). In particular, one can add a cosmological constant term, changing the integrand to $\boldsymbol{R} - \frac{8\pi\kappa}{c^2}\mu + 2\Lambda$ and the field equations to

$$\boldsymbol{R}_{\alpha\beta} - \tfrac{1}{2}\boldsymbol{R}\, g_{\alpha\beta} = -\tfrac{4\pi\kappa}{c^2}(\mu + \bar{\mu})\, g_{\alpha\beta}, \tag{5}$$

where $\frac{4\pi\kappa}{c^2}\bar{\mu} = -\Lambda$. A positive cosmological constant Λ thus appears in this context to be a (mis)representation of a negative active mass density $\bar{\mu}$ of a continuous distribution of gravitationally repulsive matter. An excess of this negative density over the positive active mass density μ of attractive matter could drive an accelerating cosmic expansion, and in doing so would provide a solution to the vexing 'Cosmological Constant Problem'. Leaving aside for the moment the question of where such a negative mass density might come from, let us explore the consequences of presuming it exists, by studying cosmological solutions of field equations that incorporate a positive mass density μ, a negative mass density $\bar{\mu}$ such that $-\bar{\mu} > \mu$, and a minimally coupled scalar field ϕ (not the newtonian ϕ). The variational principle

$$\delta \int [\boldsymbol{R} - \tfrac{8\pi\kappa}{c^2}(\mu + \bar{\mu}) + 2\,\phi^{\cdot\gamma}\phi_{.\gamma}]\, |g|^{\frac{1}{2}} d^4x = 0 \tag{6}$$

combines these elements and generates the field equations

$$\boldsymbol{R}_{\alpha\beta} - \tfrac{1}{2}\boldsymbol{R}\, g_{\alpha\beta} = T_{\alpha\beta} \coloneqq -\frac{4\pi\kappa}{c^2}(\mu + \bar{\mu})\, g_{\alpha\beta} - 2\,(\phi_{.\alpha}\phi_{.\beta} - \tfrac{1}{2}\phi^{\cdot\gamma}\phi_{.\gamma}\, g_{\alpha\beta}) \tag{7}$$

and

$$\Box\phi \coloneqq \phi^{\cdot\gamma}{}_{:\gamma} = 0. \tag{8}$$

Notice that the polarity of the coupling of ϕ to the space-time geometry, as indicated by a plus sign in Eq. (6) and a minus sign in Eq. (7), is opposite to the usual polarity. This is consistent both with Einstein's assumption and with its denial, inasmuch as the 'energy' of the scalar field included in $\phi_{.\alpha}\phi_{.\beta} - \frac{1}{2}\phi^{\cdot\gamma}\phi_{.\gamma}\, g_{\alpha\beta}$ is of a nature entirely different from that of the kinetic pressure p in Einstein's "energy-tensor".

III. COSMIC EVOLUTION EQUATIONS

For a Robertson–Walker metric $c^2dt^2 - R^2(t)ds^2$ (with t in seconds, s in centimeters, and c in cm/sec) and a dimensionless scalar field $\phi = \beta(t)$ these field equations reduce to

$$3\,\frac{\dot{R}^2/c^2 + k}{R^2} = -\frac{4\pi\kappa}{c^2}(\mu + \bar{\mu}) - \frac{\dot{\beta}^2}{c^2}, \tag{9}$$

$$\frac{2}{c^2}\frac{\ddot{R}}{R} + \frac{\dot{R}^2/c^2 + k}{R^2} = -\frac{4\pi\kappa}{c^2}(\mu + \bar{\mu}) + \frac{\dot{\beta}^2}{c^2}, \tag{10}$$

and

$$\Box\phi = \frac{1}{c^2}\left(\ddot{\beta} + 3\dot{\beta}\frac{\dot{R}}{R}\right) = 0, \tag{11}$$

where $k = 1$, 0, or -1 (strictly, $k = 1$, 0, or -1 cm^{-2}), the uniform curvature of the spatial metric ds^2. Additionally, corresponding to the identity $T_{\alpha}{}^{\beta}{}_{:\beta} = 0$, there is the equation $\frac{4\pi\kappa}{c^2}d(\mu + \bar{\mu}) = -2(\Box\phi)d\phi = 0$. If we define the 'accelerant' A by $A \coloneqq -\frac{4\pi\kappa}{c^2}(\mu + \bar{\mu})$, then $dA = 0$, so A is a constant with units cm^{-2}, positive under the assumption that $-\bar{\mu} > \mu$. This replaces the previous condition that μ is constant; it allows both μ and $\bar{\mu}$ to vary so long as their sum does not. Equation (11) yields $\dot{\beta}^2R^6 = Bc^2$, where B also is a positive constant with units cm^{-2} if, as we shall stipulate, $\dot{\beta} \neq 0$. Equations (9) and (10), which are replacements for the well-studied Friedmann cosmological equations, are then equivalent together to

$$\frac{1}{c^2}\frac{\dot{R}^2}{R^2} = -\frac{4\pi\kappa}{3c^2}(\mu + \bar{\mu}) - \frac{k}{R^2} - \frac{\dot{\beta}^2}{3c^2} \tag{12}$$

$$= \frac{A}{3} - \frac{k}{R^2} - \frac{B}{3R^6} \tag{13}$$

$$= \frac{AR^6 - 3kR^4 - B}{3R^6} =: \frac{P(R)}{3R^6} \tag{14}$$

and

$$\frac{1}{c^2}\frac{\ddot{R}}{R} = -\frac{4\pi\kappa}{3c^2}(\mu + \bar{\mu}) + \frac{2\dot{\beta}^2}{3c^2} \tag{15}$$

$$= \frac{A}{3} + \frac{2B}{3R^6} + \frac{2\dot{\beta}^2}{3c^2} \tag{16}$$

$$= \frac{AR^6 + 2B}{3R^6}. \tag{17}$$

Several properties of the scale factor R as a solution of these equations can be inferred rather easily, to wit:

- For each of $k = 1$, 0, and -1, R has a positive minimum value $R_{\rm min}$, the only positive root of the polynomial $P(R) \coloneqq AR^6 - 3kR^4 - B$, where $\dot{R} = 0$. (See Fig. 1.) This rules out a 'big bang' singularity. There is instead a 'big bounce' off a state of maximum compression at time $t = 0$, when $R(t) = R_{\rm min}$.
- $R(t)$ is symmetric about $t = 0$, and $R(t) \to \infty$ as $t \to \pm\infty$.
- $\ddot{R}$ is always positive, so the universal expansion is accelerating at all times after the bounce, and the universal contraction is decelerating at all times before the bounce.
- The 'Hubble parameter' H and the 'acceleration parameter' Q behave asymptotically as follows:

$$H \coloneqq \dot{R}/R, \quad \frac{1}{c^2}H^2 = \frac{A}{3} - \frac{3kR^4 + B}{3R^6} \to \frac{A}{3} \quad \left\{\begin{matrix}\text{from below if } k \geq 0\\ \text{from above if } k < 0\end{matrix}\right\} \text{ as } R \to \infty, \tag{18}$$

and

$$Q \coloneqq \frac{\ddot{R}/R}{(\dot{R}/R)^2} = c^2\,\frac{AR^6 + 2B}{3H^2R^6} = 1 + c^2\,\frac{kR^4 + B}{H^2R^6} \to 1 \quad \left\{\begin{matrix}\text{from above if } k \geq 0\\ \text{from below if } k < 0\end{matrix}\right\} \text{ as } R \to \infty. \tag{19}$$

Either of these entails that $R(t) \sim Ce^{\pm\sqrt{A/3}\,c\,t}$, for some constant C, as $t \to \pm\infty$.

- $\dot{H} = c^2(kR^4 + B)/R^6$, so $H(t)$ is ever-increasing if $k \geq 0$, but is at a maximum or a minimum when $R(t) = \sqrt[4]{B/(-k)}$, and is decreasing for all larger values of R, if $k < 0$.

The general formula for $R^2_{\rm min}$ in Fig. 1 is

$$R^2_{\rm min} = \frac{k}{A}\left[1 + \frac{\sqrt[3]{2}\,k}{\sqrt[3]{A^2B + 2k^3 + \sqrt{A^2B\,(A^2B + 4k^3)}}} + \frac{\sqrt[3]{A^2B + 2k^3 + \sqrt{A^2B(A^2B + 4k^3)}}}{\sqrt[3]{2}\,k}\right]. \tag{20}$$

This reduces to $R^2_{\rm min} = (B/A)^{1/3}$ when $k = 0$, and to $R^2_{\rm min} = (k/A)\,[1 - 2\cos(\theta/3)]$, where $\theta \coloneqq \pi/2 - \tan^{-1}\!\big((A^2B + 2k^3)/\sqrt{A^2B(4(-k)^3 - A^2B)}\big)$, when $k = -1$ and $A^2B < 4(-k)^3$.

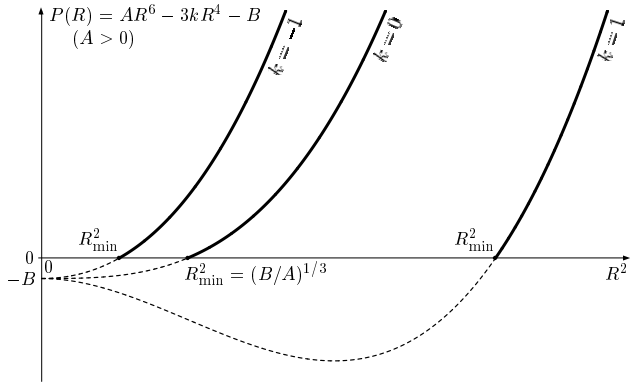

FIG. 1: Graphs of $P(R)$ versus R^2 for $k = -1$, 0, and 1, and generic values of the parameters A (> 0) and B. Only values of R for which $P(R) \geq 0$ cm^{-2} are admitted by Eq. (14).

IV. COSMOLOGICAL SOLUTIONS

A. Flat open universe ($k = 0$)

When $k = 0$, so that space is perfectly flat, $R_{\rm min} = (B/A)^{1/6}$ and it is straightforward to integrate Eqs. (14) and (17), with the result that

$$R^3(t) = R^3_{\rm min}\cosh(\sqrt{3A}\,c\,t), \tag{21}$$

from which follow

$$H(t) = c\sqrt{\frac{A}{3}}\tanh(\sqrt{3A}\,c\,t) \tag{22}$$

$$= \mathrm{sgn}(t)\,c\sqrt{\frac{A}{3}\left(1-\left[\frac{R_{\min}}{R(t)}\right]^6\right)}, \tag{23}$$

$$Q(t) = 1 + \frac{3}{\sinh^2(\sqrt{3A}\,c\,t)} \tag{24}$$

$$= 1 + \frac{3}{[R(t)/R_{\min}]^6 - 1}\,, \tag{25}$$

and

$$c^2A = H^2(t)[Q(t)+2] \tag{26}$$

$$= 3H^2(t)\left[1 + \frac{1}{[R(t)/R_{\min}]^6 - 1}\right]. \tag{27}$$

If any two of the parameters A, t_0 (the present epoch), $H(t_0)$, $Q(t_0)$, and $R(t_0)/R_{\min}$ are set, the others are fixed. Of these the only one that is reasonably well determined by observations is $H(t_0)$, which currently is estimated to be about 72 (km/sec)/Mpc. The 'big bounce' presumably should look much like a 'big bang', so the ratio $R(t_0)/R_{\min}$ should be very large, perhaps on the order of the Hubble radius $c/H(t_0)$ ($= 1.28\times10^{28}$ cm $= 13.6$ billion light years, the 'radius of the observable universe') divided by the Planck length 1.62×10^{-33} cm. With this choice $R(t_0)/R_{\min} = 7.93\times10^{60}$, which makes $Q(t_0) = 1+10^{-365}$, $c^2A = 1.63\times10^{-35}/\mathrm{sec}^2 = 1.62\times10^{-20}/\mathrm{yr}^2$, and $t_0 = 1.91\times10^{12}$ years. This value for t_0 encompasses 140 of the 13.6×10^9 years predicted to have elapsed since the 'big bang' by the 'standard' (or 'concordance') model based on the Friedmann–Robertson–Walker (FRW) equations, an interval which in the present instance would allow approximately only a doubling from $R_{\min}$ to $R(t)$.

B. Closed universe ($k = 1$)

When $k = 1$ (strictly, $k = 1$ cm^{-2}), so that space is an expanding 3-sphere (contracting before the bounce), $R_{\min}^2$ is bounded below by its limit as $B \to 0$, which is $3k/A$. Indeed, the field equations have a bounce solution with $B = 0$ and $R_{\min} = \sqrt{3k/A}$, given by

$$R(t) = R_{\min}\cosh\left(\sqrt{A/3}\,c\,t\right). \tag{28}$$

This is a pure de Sitter model with $Q(t) = 1$,

$$H(t) = c\sqrt{\frac{A}{3}}\tanh(\sqrt{A/3}\,c\,t) \tag{29}$$

$$= \mathrm{sgn}(t)\,c\sqrt{\frac{A}{3}\left(1-\left[\frac{R_{\min}}{R(t)}\right]^2\right)}, \tag{30}$$

and

$$c^2A = \frac{3H^2(t)}{1-[R_{\min}/R(t)]^2}. \tag{31}$$

Using $H(t_0) = 72$ (km/sec)/Mpc and $R(t_0)/R_{\min} = 7.93\times10^{60}$ as above, one calculates that $c^2A = 1.62\times10^{-20}/\mathrm{yr}^2$, $t_0 = 1.92\times10^{12}$ years, $R_{\min} = 1.28\times10^{28}$, and $R(t_0) = 1.02\times10^{89}$. Thus in this model, where it is meaningful to speak of the 'radius of the universe', that radius at the time of the bounce is $R_{\min}/\sqrt{k} = 1.28\times10^{28}$ cm $= 13.6$ billion light years (the Hubble radius), and the radius at the present epoch is 1.01×10^{71} light years. For $B \neq 0$ the radius at the bounce will be larger.

C. Nonflat open universe ($k = -1$)

The remaining case is the most interesting of the three. When $k = 0$ or 1, H is an increasing function of R and therefore, post bounce, of t, rising leisurely to its asymptotic value $c\sqrt{A/3}$. When $k = -1$ (cm^{-2}), the situation is quite different, as the graphs in Fig. 2 demonstrate. Here $H(R)$ has a maximum value

$$H_{\max} = c\sqrt{\frac{A}{3} + \frac{2\,(-k)^{3/2}}{3\sqrt{B}}} \tag{32}$$

at $R = \sqrt[4]{B/(-k)} =: R_{H_{\max}}$, where $dH/dR = c^2(kR^4 + B)/H(R)R^7 = 0$. Now H rises sharply from 0 at $R_{\min}$ to $H_{\max}$ at $R_{H_{\max}}$, then reverses and tails off asymptoticlly to $c\sqrt{A/3}$. One can show that $R_{\min} \sim \sqrt[4]{B/3(-k)}$ as $B \to 0$. Thus as $B \to 0$, $R_{H_{\max}}$ and $R_{\min}$ are squeezed together, and $H_{\max}$ grows without bound. This clearly is a recipe for an explosive post-bounce inflation followed by a deceleration-mimicking decline in H. That the decline in H mimics a deceleration of the expansion is borne out by the behavior of Q as reflected in Fig. 3. Descending from ∞ at $R_{\min}$, $Q(R)$ passes through 1 at $R_{H_{\max}}$, bottoms out with a minimum value $Q_{\min}$ at $R_{Q_{\min}}$, where

$$R_{Q_{\min}} = \sqrt[6]{\frac{B}{A}}\sqrt{\sqrt[3]{2+\sqrt{4-A^2B/(-k)^3}} + \frac{\sqrt[3]{A^2B/(-k)^3}}{\sqrt[3]{2+\sqrt{4-A^2B/(-k)^3}}}}\,, \tag{33}$$

then creeps slowly back to 1 as $R \to \infty$. One sees that, as $B \to 0$, $R_{Q_{\min}} \sim \sqrt[6]{4B/A} = \sqrt[6]{4(-k)/A}\, R_{H_{\max}}^{2/3}$, so $R_{Q_{\min}}$ goes to 0 along with $R_{H_{\max}}$ and $R_{\min}$, but lagging behind somewhat.

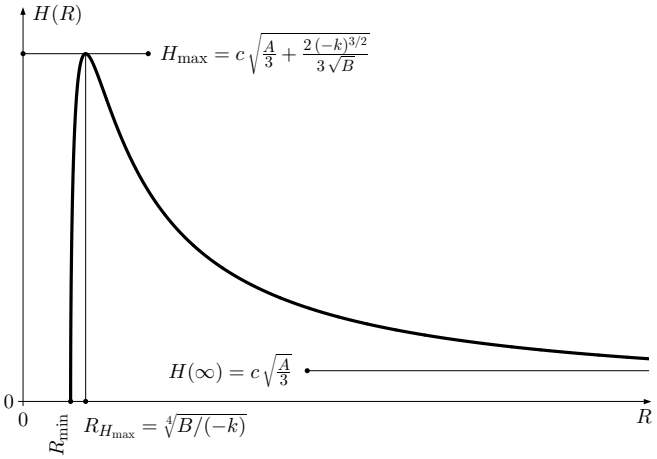

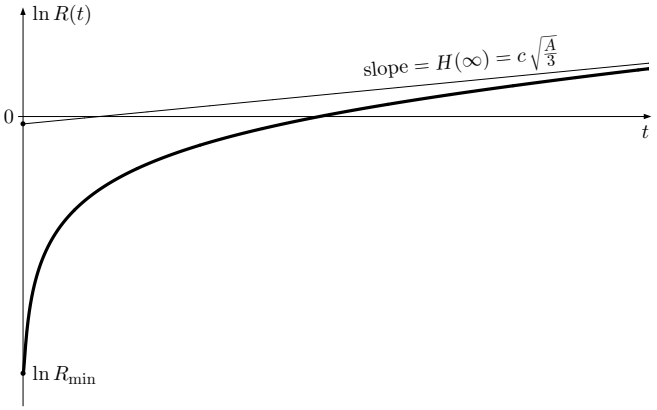

FIG. 2: Graphs of $H(R)$ and $\ln R(t)$ for $k = -1$ and generic values of the parameters A (> 0) and B, showing early stage inflation followed by a deceleration-mimicking decline in H. The functions are related by $(\ln R)\dot{}(t) = \dot{R}(t)/R(t) =: H(R(t))$.

Numerical investigation of the $k = -1$ model can be carried out by use of the Mathematica program described in Appendix A, which takes as inputs $H(t_0)$, $H_{\max}$, and $Q(t_0)$ to fix A, B, and $R(t_0)$, then solves for the normalized scale factor $S \coloneqq R/R_{\min}$ the equation, equivalent to Eq. (17),

$$\ddot{S} = \frac{c^2 A}{3} S + \frac{2c^2 B/3R_{\min}^6}{S^5}, \tag{34}$$

with initial conditions $S(0) = 1$ and $\dot{S}(0) = 0$ at the bounce. Solution in hand, one can compute various parameters of interest. Included in Appendix A is a sample run of the program with inputs $H(t_0) = 72$ (km/sec)/Mpc, $H_{\max} = (5 \times 10^{60}) H(t_0)$, and $Q(t_0) = 1/2$, which produces the solution $S(t)$ represented in Fig. 4. The program computes algebraically

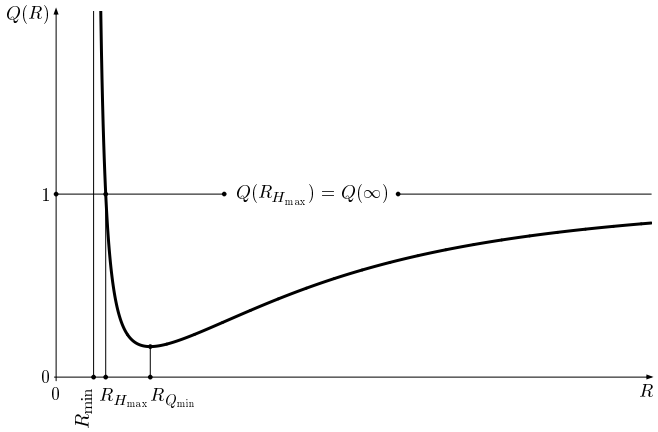

FIG. 3: Graph of the acceleration $Q(R)$ for $k = -1$ and generic values of the parameters A (> 0) and B, showing large early acceleration followed by a deceleration-mimicking descent to a minimum acceleration at $R_{Q_{\min}}$ and asymptotic rise to a de Sitter acceleration $Q(\infty) = 1$.

that $A = 9.09 \times 10^{-57}/\mathrm{cm}^2$, $B = 1.94 \times 10^{-131}/\mathrm{cm}^2$, $R_{\min} = 1.59 \times 10^{-33}$, $R(t_0) = 1.82 \times 10^{28}$, $R(t_0)/R_{\min} = 1.14 \times 10^{61}$, and $Q_{\min} = 9.28 \times 10^{-82}$. Integration of Eq. (34), which now reads

$$\ddot{S} = (2.72 \times 10^{-36}/\mathrm{s}^2) S + \frac{7.19 \times 10^{86}/\mathrm{s}^2}{S^5}, \tag{34$'$}$$

shows that $t_0 = 5.34 \times 10^{17}$ seconds $= 16.9$ billion years and that the time t of one hundred doublings (when $R(t)/R_{\min} = S(t) = 2^{100}$) is 6.74×10^{-14} seconds. These times appear to be within the rough boundaries described by Guth in [8].

Table I in Appendix B gives results from thirty-five runs of the program with various choices of $H_{\max}$ and $Q(t_0)$, keeping $H(t_0) = 72$ (km/sec)/Mpc. As is apparent there, increasing $H_{\max}$ shortens the time from the bounce to the end of inflation and the transition to uphill coasting shown in Fig. 4, with little effect on t_0 and the time of return from coasting to exponential expansion, whereas varying $Q(t_0)$ alters t_0 and the time of transition from coasting to exponential expansion, but has little effect on the timing of the end of inflation and the onset of coasting. Whatever the inputs, the pre-bounce evolution is a mirror image of the post-bounce, comprising exponential contraction and downhill coasting to rapid deflation into the bounce.

D. Solutions with $A \leq 0$ ($-\bar{\mu} \leq \mu$)

The preceding models are predicated on the supposition that $-\bar{\mu} > \mu$, but $-\bar{\mu} = \mu$ and $-\bar{\mu} < \mu$ are also possibilities to be considered. When $-\bar{\mu} = \mu$, so that $A = 0$, the polynomial $P(R)$ has a positive root only if $k = -1$, namely, $R = R_{\min} \coloneqq \sqrt[4]{B/3(-k)}$. The generic behaviors of $H(R)$ and $R(t)$ are as shown in Fig. 2 with

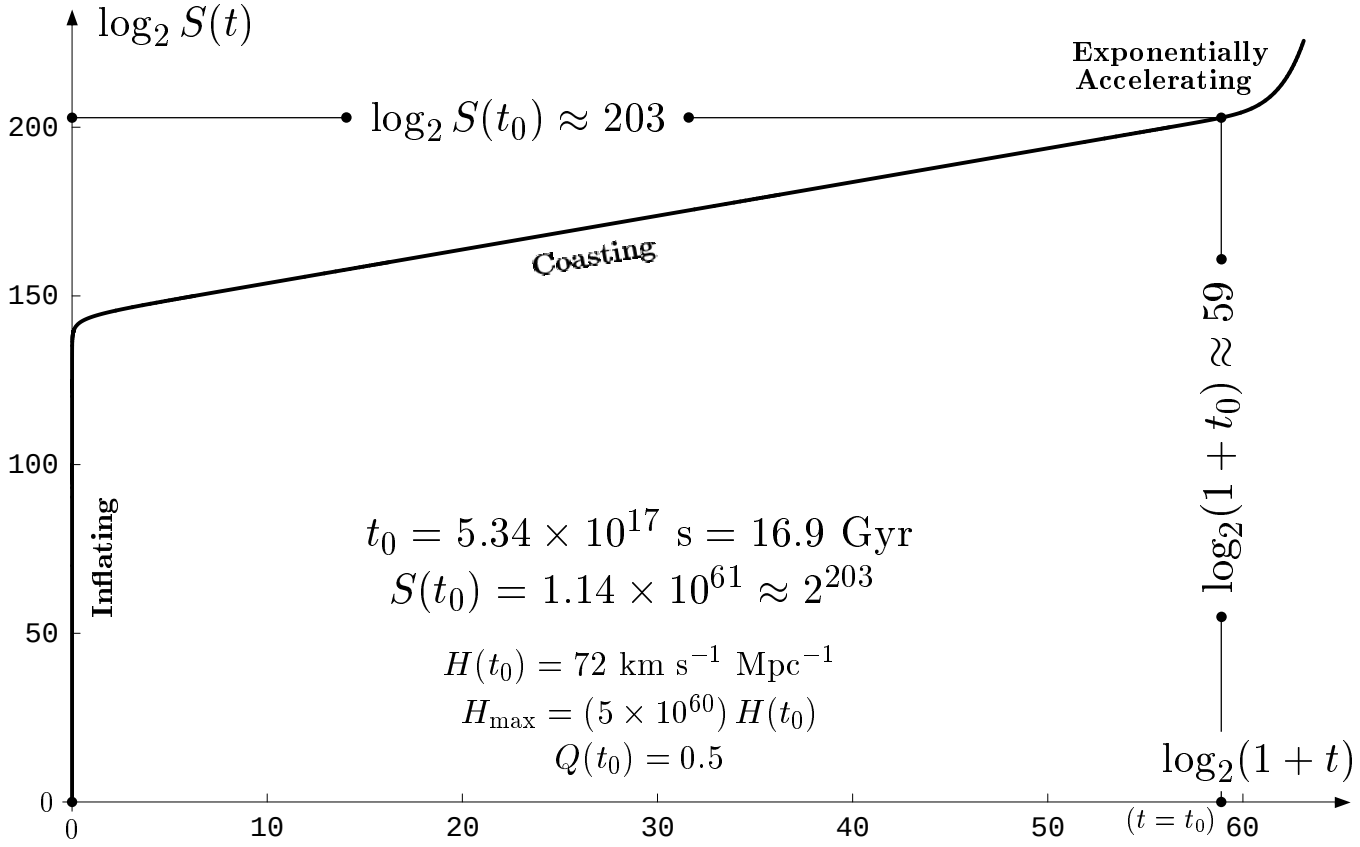

FIG. 4: Graph of $\log_2 S(t)$ versus $\log_2(1+t)$ for the sample solution of Appendix A. The early stage rapid inflation, after producing approximately 144 doublings of the normalized scale factor S in about one second, gives way to a long period of uphill 'coasting' (where the graph is nearly linear), followed by a return to exponential acceleration after $t = t_0$. In the coasting period $\log_2 S(t) \approx 144 + ((203-144)/(59-0))\log_2(1+t) = 144 + \log_2(1+t)$, so $S(t) \approx 2^{144}(1+t)$, making the expansion essentially linear with time. As seen in Table I, reducing $Q(t_0)$ to 0.01 shortens t_0 to 13.6 Gyr.

$A = 0$, except that the graph of $\ln R(t)$ has no linear asymptote, rather is asymptotic to $\ln(\sqrt{-k}\,c\,t)$ as $t \to \infty$. Unlike the behavior in Fig. 3, $Q(R)$ has no minimum, instead decreases asymptotically to 0 as $R \to \infty$. A sample run of a modified version of the program in Appendix A, with $A = 0$, $H(t_0) = 72$ (km/sec)/Mpc, and $H_{\max} = (5\times10^{60})H(t_0)$ as inputs, produces the same values for B, $R_{\min}$, and the hundred-doublings time as in the previous sample run, and yields $t_0 = 4.3\times10^{17}$ seconds = 13.6 billion years, $R(t_0) = 1.3\times10^{28}$, $R(t_0)/R_{\min} = 8.1\times10^{60}$, and $Q(t_0) = 4.7\times10^{-244}$. The graph analogous to that of Fig. 4 looks the same except that the coasting era goes on forever, with no return to exponential expansion.

When $-\bar{\mu} < \mu$, so that $A < 0$, $P(R)$ has a real root only if $k = -1$ and $A^2B \le 4(-k)^2$. When $A^2B < 4(-k)^2$ there are two positive roots, $R_{\min}$ and $R_{\max}$, given by $R^2_{\min} = (k/A)[1+\cos(\theta/3) - \sqrt{3}\sin(\theta/3)]$ and $R^2_{\max} = (k/A)[1+\cos(\theta/3) + \sqrt{3}\sin(\theta/3)]$, where $\theta := \pi/2 - \tan^{-1}\big((A^2B+2k^3)/\sqrt{-A^2B(A^2B+4k^3)}\big)$. These reduce to a single root $R = R_0 := \sqrt{2k/A}$ when $A^2B = 4(-k)^2$, as seen in Fig. 5. In the latter case, because $P(R)$ is negative for all positive values of R other than R_0, the solution of the field equations is simply $R(t) = R_0$, which makes a static, open universe, with negative spatial curvature k/R_0^2.

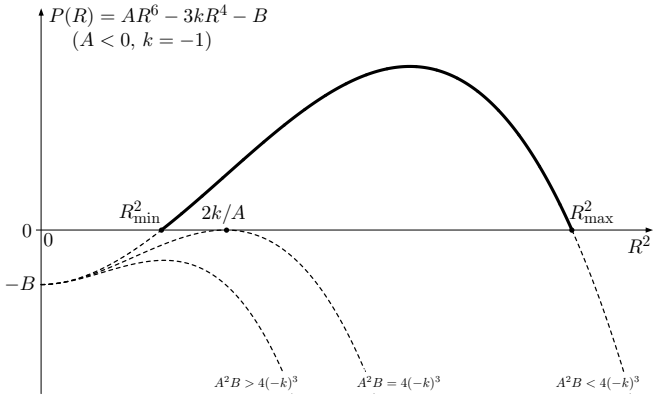

FIG. 5: Graphs of $P(R)$ versus R^2 for $k = -1$ and generic values of the parameters A (< 0) and B. Only values of R for which $P(R) \ge 0$ cm^{-2} are admitted by Eq. (14).

For the case of two positive roots the behaviors of $H(R)$

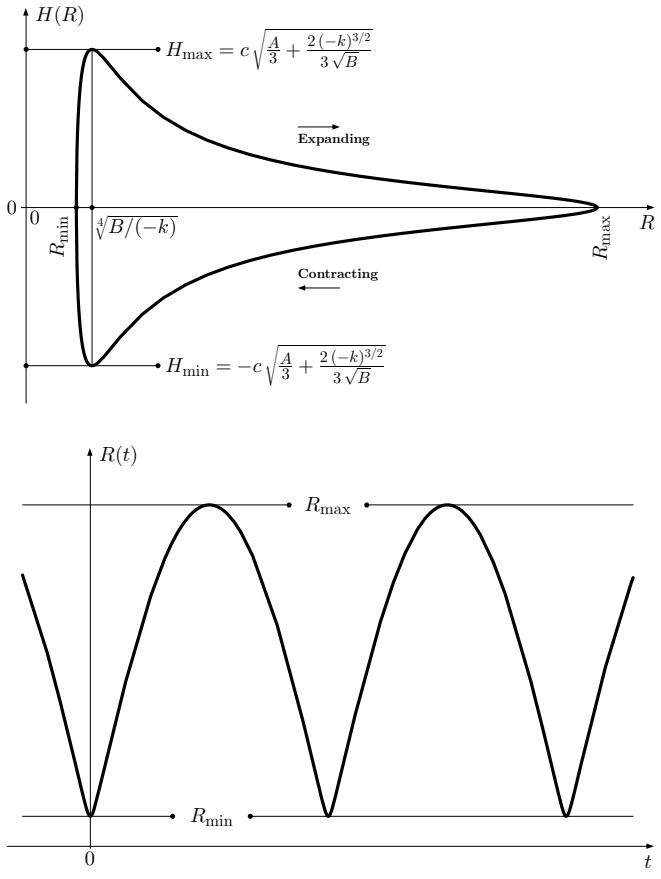

FIG. 6: Graphs of $H(R)$ and $R(t)$ for $k = -1$ and generic values of the parameters A (< 0) and B satisfying $A^2B < 4(-k)^3$, showing repetitive, identical periods of expansion and contraction, each beginning with a stage of rapid inflation from a bounce at $R = R_{\min}$, which is followed by a less rapid expansion to $R = R_{\max}$, then a mirror-image contraction to an ending stage of rapid deflation into the next bounce at $R = R_{\min}$. The functions are related by $\dot{R}(t)/R(t) =: H(R(t))$.

and $R(t)$ are shown in Fig. 6. The universe modeled is a periodic universe, 'breathing' much as marine mammals breathe when diving: inhaling by rapidly inflating their lungs, holding the breath for a long interval, then exhaling by rapidly deflating the lungs to repeat the cycle. A sample run of a modified version of the program in Appendix A, starting from a bounce with $H(t_0) = 72$ (km/sec)/Mpc, $H_{\max} = (5 \times 10^{60})H(t_0)$, and $Q(t_0) = 0$, produces $A = -8.1 \times 10^{-300}/\text{cm}^2$ and $B = 1.9 \times 10^{-131}/\text{cm}^2$, and yields results essentially the same as those of the sample run for $A = 0$, with the addition that $S_{\max} \coloneqq R_{\max}/R_{\min} = 3.7 \times 10^{182}$. A run starting from a 'bounce off the ceiling' ($S(0) = S_{\max}$ and $\dot{S}(0) = 0$) with the same inputs shows the length of a cycle to be about 6.2×10^{139} seconds, which is 2.0×10^{132} years, the vast majority of which is spent coasting: for 6.0×10^{139} of those seconds $S(t) > 1.7 \times 10^{181}$ and $|H(t)| < 3.4 \times 10^{-119}$ (km/sec)/Mpc.

V. DARK MATTER AND DARK 'ENERGY'

A. Drainholes

Having examined all the cosmological models of Robertson–Walker type that obey the modified field equations (7) and (8) with a negative active gravitational mass density $\bar{\mu}$ incorporated, let us turn now to the task of identifying a source for that density. As it happens, there is ready to hand a candidate that fits well into the present context. In 1973 I described in considerable detail a model of a gravitating particle alternative to the Schwarzschild vacuum solution of Einstein's field equations. This space-time manifold, which I termed a 'drainhole' with 'ether' flowing through it, was discovered independently at about the same time by Bronnikov, has subsequently come to be recognized as an early (perhaps the earliest) example of what is now called by some a 'traversable wormhole', and has been analyzed from various perspectives by others [9–15]. The metric is a static, spherically symmetric solution of the field equations (7) and (8) with $\mu = \bar{\mu} = 0$. (N.B. $\boldsymbol{R}_{\alpha\beta}$ and $\boldsymbol{R}$ here are the negatives of those in [9].) It has the proper-time forms (in units in which $c = 1$)

$$d\tau^2 = [1 - f^2(\rho)]\, dT^2 - [1 - f^2(\rho)]^{-1}\, d\rho^2 - r^2(\rho)\, d\Omega^2 \tag{35}$$

$$= dt^2 - [d\rho - f(\rho)\, dt]^2 - r^2(\rho)\, d\Omega^2, \tag{36}$$

where $t = T - \int f(\rho)[1 - f^2(\rho)]^{-1}\, d\rho$,

$$f^2(\rho) = 1 - e^{-(2m/n)\alpha(\rho)}, \tag{37}$$

$$r(\rho) = \sqrt{(\rho - m)^2 + a^2}\, e^{(m/n)\alpha(\rho)}, \tag{38}$$

and

$$\phi = \alpha(\rho) = \frac{n}{a}\left[\frac{\pi}{2} - \tan^{-1}\left(\frac{\rho - m}{a}\right)\right], \tag{39}$$

and $a \coloneqq \sqrt{n^2 - m^2}$, the parameters m and n satisfying $0 \le m < n$. (The coordinate ρ used here translates to $\rho + m$ in [9].) The shapes and linear asymptotes of r and f^2 are shown in Fig. 7. Not shown, but verifiable, is that $f^2(\rho) \sim 2m/\rho$ as $\rho \to \infty$, which shows m to correspond to the Schwarzschild mass parameter.

The choke point of the drainhole throat is the 2-sphere at $\rho = 2m$, of radius $r(2m)$, which increases monotonically from n to ne as m increases from 0 to n. Thus the size of the throat is determined almost exclusively by n, independently of m. Although the scalar field ϕ has a nonkinetic 'energy' density that contributes to the space-time curvature through $T_{\alpha\beta}$, this energy has little to do with the strength of gravity (as determined by m), rather is associated with negative spatial curvatures found in the open throat, the negativity of which

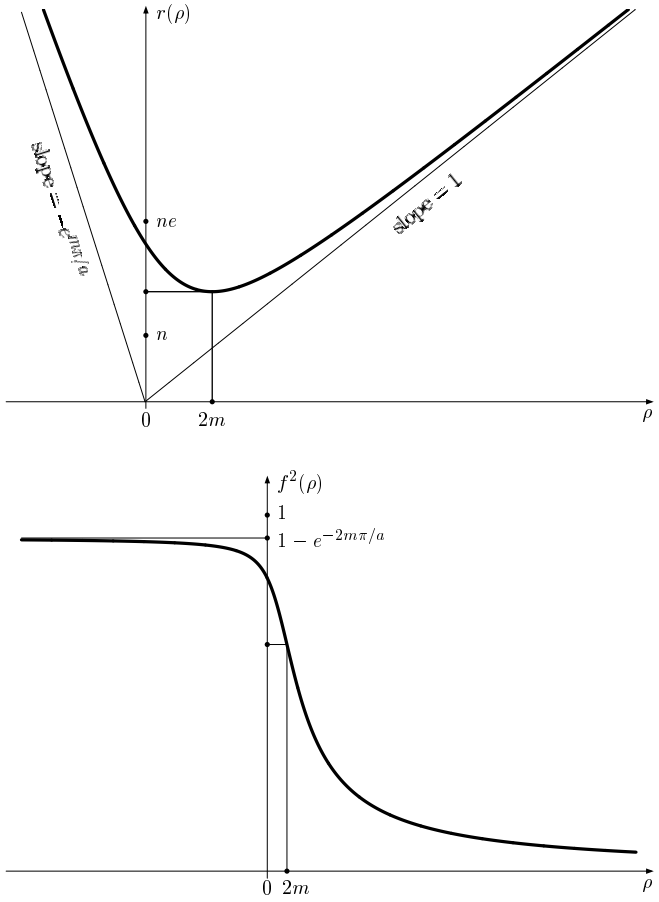

FIG. 7: Graphs of $r(\rho)$ and $f^2(\rho)$ for generic values of the parameters m and n.

mandates the nonstandard polarity of the coupling as expressed by a minus sign in $T_{\alpha\beta}$ in Eq. (7). As a matter of perspective, it is more insightful to consider that the scalar field does not *cause* (i.e., is not a source of) these spatial curvatures, but simply tells of their existence and describes their configuration. This perspective helps disabuse one of the peculiar notion that geometrically unexceptionable space-time manifolds such as the drainhole are somehow a product of 'exotic' matter just because their Ricci tensors disrespect some 'energy condition'. Moreover, it is not a great stretch to surmise that, whereas the parameter m specifies the active gravitational mass of the (nonexotic) drainhole particle, the size parameter n specifies in some way its inertial rest mass. This speculation is supported by two considerations: first, as shown in [9], the total energy of the scalar field ϕ lies in the interval from $n/2$ to $n\pi/2$, thus is essentially proportional to n; second, it would seem likely that the bigger the hole, the greater the force needed to move it.

Because $r(\rho) \geq n > 0$ and $f^2(\rho) < 1$, the drainhole space-time manifold is geodesically complete and has no one-way event horizon, the throat being therefore traversable by test particles and light in both directions. The manifold is asymptotic as $\rho \to \infty$ to a Schwarzschild manifold with (active gravitational) mass parameter m. The flowing 'ether' (a figurative term for a cloud of inertial observers free-falling geodesically from rest at $\rho = \infty$) has radial velocity $f(\rho)$ (taken as the negative square root of $f^2(\rho)$) and radial acceleration $(f^2/2)'(\rho)$, which computes to $-m/r^2(\rho)$ and therefore is strongest at $\rho = 2m$. Because the radial acceleration is everywhere aimed in the direction of decreasing ρ, the drainhole attracts test particles on the high, front side, where $\rho > 2m$, and repels them on the low, back side, where $\rho < 2m$. Moreover, the manifold is asymptotic as $\rho \to -\infty$ to a Schwarzschild manifold with mass parameter $\bar{m} = -me^{m\pi/a}$, so the drainhole repels test particles more strongly on the low side than it attracts them on the high side, in the ratio $-\bar{m}/m = e^{m\pi/\sqrt{n^2-m^2}}$. The drainhole is a kind of natural accelerator of the 'gravitational ether', drawing it in on the high side and expelling it more forcefully on the low side. To replace the somewhat disreputable term 'ether' with something more acceptable in polite society one can imagine that it is space itself that is flowing into the drainhole and out the other end. This should cause no alarm, for the very notion of an expanding universe already imputes to space the requisite plasticity.

The discovery of the drainhole manifolds arose, in my case, from a search for a model for gravitating particles that, unlike a Schwarzschild space-time manifold, would have no singularity. Geodesic completeness and absence of event horizons followed naturally from that requirement. As shown in [9], a drainhole possesses all the geodesic properties that a Schwarzschild blackhole possesses other than those that depend on the existence of its horizon and its singularity, having eliminated the horizon and replaced the singularity with a topological passageway to another region of space. Drainholes are able, therefore, to reproduce all the externally discernible aspects of physical blackholes that Schwarzschild blackholes reproduce. That their back sides have never been recognizably observed (but in principle could be), is no more troubling than the impossiblity of directly observing the back sides of Schwarzschild horizons. For these reasons drainholes are more satisfactory than Schwarzschild blackholes as mathematical models of centers of gravitational attraction. Moreover, there is little reason to doubt that rotating drainhole manifolds analogous to the Kerr rotating blackhole manifolds exist and will prove to be better models than the Kerr manifolds. (A recent solution of the field equations (7) and (8) perhaps describes such a manifold [16].)

B. Dark matter and dark 'energy' from drainholes

A physical center of attractive gravity modeled by a drainhole would qualify to be called a 'darkhole', inasmuch as (as shown in [9]) it would capture photons and other particles that venture too close, but, unlike a blackhole, must eventually release them, either back to the

attracting high side whence they came or down through the drainhole and out into the repelling low side. Thus one can imagine that at galactic centers will be found not supermassive blackholes, but supermassive darkholes instead. This, however, is not the end of the story. A central tenet of the general theory of relativity is that every elementary object that 'has gravity' is a manifestation of a local departure of the geometry of space-time from flatness. If such an object has other properties ascribed to it by quantum theory, these must be additional to the underlying geometrical structure. I therefore propose the hypothesis that every such elementary gravitating object is at its core an actual physical drainhole — these objects to include not only elementary constituents of visible matter such as protons and neutrons, or, more likely, quarks, but also the unseen particles of 'dark matter' whose existence is at present only inferential. Those drainholes associated with visible matter I will call 'bright drainholes', those not so associated, 'dark drainholes'.

The pure, isolated drainhole described by Eqs. (35–39) is an 'Einstein–Rosen bridge' between two otherwise disjoint 'subuniverses' each of which by itself would for its description consume all the resources of a Robertson–Walker metric. Nonisolated drainholes could presumably exist not only as 'bridges' between our subuniverse and another, but also as 'tunnels', with both their entrances and their exits in our subuniverse. Both types could contribute to the negative mass density $\bar{\mu}$ as well as to μ, the bridge drainholes contributing to $\bar{\mu}$ if their gravitationally repulsive back sides reside in our subuniverse, the tunnel drainholes contributing to $\bar{\mu}$ by way of their gravitationally repulsive exits. Tunnel drainholes are easy enough to visualize in abundance as topological holes into which space disappears, only to reappear elsewhere, in analogy with rivers that go underground and surface somewhere downstream. Existence of an abundance of bridge drainholes with their back sides all resident in our subuniverse requires a more complex visualization. At one extreme each of their front sides might be resident in its own subuniverse distinct from those of the others. At the other extreme their front sides might all reside together in one subuniverse. Between these extremes there could be groups of various sizes, those in each group sharing a subuniverse. If one invokes these bridge drainholes to supply a part of the negative mass density $\bar{\mu}$, then one is faced with the question of how their various subuniverses got 'close enough' to ours to allow the bridges to form. Moreover, the magnitude of the density $\bar{\mu}$ that they produced would seem to depend on circumstances in those other subuniverses, circumstances beyond our ken. Neither of these questions arises in the case of tunnel drainholes. I shall, therefore, assume that no bridge drainholes contribute to $\bar{\mu}$, that the only possible contributors are tunnel drainholes.

Lacking for the present a full mathematical description of these tunnel drainholes, let us nevertheless proceed as if they exist and are characterized by parameters m and n related as in an isolated bridge drainhole. We can then consider our (sub)universe to be populated with both tunnel drainholes and the high, front sides of bridge drainholes (call them 'bridgefronts'), bright ones associated with visible, baryonic matter, dark ones not so associated, these drainholes to provide all the gravity, attractive or repulsive, to be found in our (sub)universe. It then becomes a question of sorting the bright and the dark into tunnels and bridgefronts. The simplest sorting that will suit our purposes is to identify the bright drainholes with the bridgefronts and the dark drainholes with the tunnels. (An exception might be required for galactic centers. Their backsides could be made highly visible by light that falls into the front sides and out the back. If they are bridgefronts, they would be visible, but only in the different subuniverses their backsides reside in; that would make them dark bridgefronts. If they are tunnels, their backsides would be visible in our subuniverse; that would make them bright tunnels. Because the masses at the centers of galaxies are only a small fraction of the total masses of the galaxies, such drainholes at galactic centers, if extant, are ignorable for present purposes.)

Let us then examine a universe represented by any one of the solutions discussed above, populated with drainholes, the bright bridgefronts associated with visible, baryonic matter, the dark tunnels not, and distributed with an attractive gravitational mass density μ and a repulsive density $\bar{\mu}$, which combine to produce the accelerant A. What can we say about μ and $\bar{\mu}$? Split μ into $\mu = \mu_{\rm B} + \mu_{\rm D}$ (B for bright bridgefronts, D for dark tunnels). Then $\bar{\mu}_{\rm B} = 0$ (in our subuniverse) and from $A = -\frac{4\pi\kappa}{c^2}(\mu + \bar{\mu}) = -\frac{4\pi\kappa}{c^2}(\mu_{\rm B} + \mu_{\rm D} + \bar{\mu}_{\rm D})$ follows $-\bar{\mu}_{\rm D}/\mu_{\rm D} = 1 + \mu_{\rm B}/\mu_{\rm D} + c^2A/4\pi\kappa\mu_{\rm D}$. If we assume that at each epoch the dark tunnels all have the same mass and size parameters m and n, then $-\bar{\mu}_{\rm D}/\mu_{\rm D} = -\bar{m}/m = e^{m\pi/a}$, so that $m/\sqrt{n^2 - m^2} = m/a = \ln(-\bar{\mu}_{\rm D}/\mu_{\rm D})/\pi = \ln(1 + \mu_{\rm B}/\mu_{\rm D} + c^2A/4\pi\kappa\mu_{\rm D})/\pi$. This entails that

$$\left(\frac{m}{n}\right)^2 = \frac{[\ln(1 + \mu_{\rm B}/\mu_{\rm D} + c^2A/4\pi\kappa\mu_{\rm D})]^2}{\pi^2 + [\ln(1 + \mu_{\rm B}/\mu_{\rm D} + c^2A/4\pi\kappa\mu_{\rm D})]^2}\,. \quad (40)$$

Because it is only the combination $-\frac{4\pi\kappa}{c^2}(\mu_{\rm B} + \mu_{\rm D} + \bar{\mu}_{\rm D})$ that remains constant, it is possible for the densities $\mu_{\rm B}$ and $\mu_{\rm D}$ to change over time in some arbitrary fashion if $\bar{\mu}_{\rm D}$ changes to compensate. Indeed $\mu_{\rm D}$ might not change at all, which would require 'continuous creation' of dark tunnels to hold that density constant in the expanding universe. In that case $\mu_{\rm D}$ would be the density of cold dark matter at the present epoch, which is estimated to be about 22% of the critical density $\mu_{\rm c}$ of the FRW standard model: $\mu_{\rm c} = 3H^2(t_0)/8\pi\kappa = 9.7 \times 10^{-30}\,{\rm g/cm^3}$. The density $\mu_{\rm B}$ of gravitating nuclear matter, on the other hand, would be expected to have grown from its pre-nucleosynthesis value of 0 to its value at the present epoch, estimated to be about 4% of $\mu_{\rm c}$. Thus the ratio $\mu_{\rm B}/\mu_{\rm D}$ would have increased from 0 to 4/22 in the interval from $t = 0$ to $t = t_0$. For all the models de-

tailed above that have $A > 0$, $H(t_0) = c\sqrt{A/3}$ to a very close approximation, which makes $c^2A/4\pi\kappa\mu_{\rm D} = 3H^2(t_0)/4\pi\kappa(0.22\mu_{\rm c}) = 2/0.22 = 9.09$. Equation (40) then shows m/n increasing from 0.593 when $\mu_{\rm B}/\mu_{\rm D} = 0$ to 0.596 when $\mu_{\rm B}/\mu_{\rm D} = 4/22$. If n is the Planck length, then, rounded off, $m = 0.60 \times \left(1.6 \times 10^{-33}\,{\rm cm}\right)$, which is 1.3×10^{-5} grams (= 0.60 Planck mass) in units in which $c = \kappa = 1$. This has the dark tunnel particles gravitating (*not* 'weighing') much more than protons and neutrons, and antigravitating ten times as much as that $\left(-\bar{m}/m = \exp\left[(m/n)\pi/\sqrt{1-(m/n)^2}\,\right] = 10.6\right)$. To maintain the density $\mu_{\rm D}$ these tunnel particles would have to be created at a rate that would keep on average one of their entrances in every 6×10^9 cubic kilometers, which would keep the entrances on average about 1800 kilometers apart. A recently reported study of dwarf spheroidal satellite galaxies of the Milky Way found that they have a maximum central dark matter density of approximately $5 \times 10^8 M_\odot/{\rm kpc}^3 = 3.4 \times 10^{-23}\,{\rm g/cm}^3 = 1.6 \times 10^7 \mu_{\rm D}$ [17]. This density corresponds to a dark tunnel entrance distribution of one per 384 cubic kilometers on average, and a mean separation of seven kilometers. To decrease the mass m and thereby increase these number densities would require taking n smaller than the Planck length.

Now consider the other extreme, in which instead of the density $\mu_{\rm D}$ staying fixed, the total active gravitational mass of the dark matter is unchanging, so that $\mu_{\rm D}$ decreases in inverse proportion to the cube of the scale factor R: thus $\mu_{\rm D} = \mu_{{\rm D},t\,=\,t_0}\,[R(t_0)/R(t)]^3$. Equation (40) now reads

$$\left(\frac{m}{n}\right)^2 = \frac{\left[\ln(1 + \mu_{\rm B}/\mu_{\rm D} + (c^2A/4\pi\kappa\mu_{{\rm D},t\,=\,t_0})\,[R(t)/R(t_0)]^3)\right]^2}{\pi^2 + \left[\ln(1 + \mu_{\rm B}/\mu_{\rm D} + (c^2A/4\pi\kappa\mu_{{\rm D},t\,=\,t_0})\,[R(t)/R(t_0)]^3)\right]^2}\,. \tag{41}$$

If from the end of nucleosynthesis onward the total active gravitational mass of baryonic matter stays fixed, then during that interval $\mu_{\rm B} = \mu_{{\rm B},t\,=\,t_0}\,[R(t_0)/R(t)]^3$, so $\mu_{\rm B}/\mu_{\rm D} = \mu_{{\rm B},t\,=\,t_0}/\mu_{{\rm D},t\,=\,t_0} = 4/22$. Before nucleosynthesis $\mu_{\rm B}/\mu_{\rm D} = 0$. Here the ratio of m to n increases as t goes from 0 to ∞, and does so monotonically in the post-nucleosynthesis era. When $t = 0$, $m/n = 4.6 \times 10^{-183}$. When $t = t_0$, $m/n = 0.596$ as in the continuous creation case. As $t \to \infty$, $m/n \to 1$ and $-\bar{m}/m \to \infty$ (the flow of the 'gravitational ether' through the tunnels grows asymptotically to the maximum rate that the tunnels can accommodate). In contrast to the continuous creation version, which drives the accelerating expansion by continually producing new tunnel drainholes of fixed size and mass, this version drives it by continuously increasing the masses of a fixed population of tunnel drainholes of common size parameter n. A mixture of the two modes could produce the same accelerant and therefore the same acceleration. And in neither case is it carved in stone that the sizes must be uniform or constant in time — only the ratio of m to n is determinate. Indeed, for a fixed population of tunnels n would presumably have to have been at the time of the bounce much less than the Planck length, for at that time all of the tunnels now present in the observable universe would have been confined to a region whose radius was the Planck length.

For the model with $A = 0$, and the ratio $\mu_{\rm B}/\mu_{\rm D}$ growing from 0 at $t = 0$ to 4/22 at $t = t_0$, Eq. (40) shows m/n growing from 0 to 0.0531 in both the continuous creation and the constant $\mu_{\rm D}$ modes. If n is the Planck length, then at the present epoch $m = 1.2 \times 10^{-6}$ grams, which gives an overall particle number density of one per 6×10^8 cubic kilometers, and a dwarf spheroidal central number density of one per 35 cubic kilometers, with $-\bar{m}/m = 1.18$. For the model with $A = -8.1 \times 10^{-300}/{\rm cm}^2$ the numbers are essentially the same.

From these considerations it is apparent that tunnel drainholes in and of themselves can serve simultaneously as the unseen 'dark matter' and the mysterious 'dark energy' whose existences current cosmological observations demand. But this raises another interesting question: If dark matter, which has recently been conclusively tied to the galaxies in galactic clusters [18], consists of the gravitationally attractive entrances of tunnel drainholes, where do the repulsive exits of these tunnels congregate? To represent such tunnels the simple model of Eqs. (35–39) would need modifying to one in which the entrance and the exit both lie in our subuniverse. It ought also be dynamical, to allow a tunnel to arise where none was before, and to let the ends of the tunnel migrate. Not having in hand such a mathematical model as a solution of field equations, one is reduced to qualitative speculations based on the presumption that one exists, as follows. (A simple nongravitating drainhole with a dynamical aspect is described in [19].) If at some point in space a strong local concentration of spatial curvature (a 'quantum fluctuation', say) should develop, a tunnel drainhole might form, through which might begin to flow the gravitational 'ether' (or, one could equally well say, as noted above, space itself, inasmuch as expansion of the universe imputes to space a certain degree of liveliness). The entrance and the exit of this newly created two-sided particle, if close together in the ambient space, would drift apart as the exit repelled the entrance more strongly than the entrance attracted the exit. Apply this to a multitude of such particles and you will likely see the entrances being brought together by both their mutual attractions and the repulsion from the exits. The exits, on the other hand, would repel one another and would tend, therefore, to spread themselves more or less uniformly over regions

from which they had expelled the entrances. Herein lies a mechanism for creating the voids, walls, filaments, and nodes of the observed universe, thus explaining the 'void phenomenon' described by Peebles without resorting to the "perhaps desperate idea ... that the voids have been emptied by the growth of holes in the [active gravitational] mass distribution" [20]. What is more, the walls, filaments, and nodes so created would likely be, in agreement with observation, more compacted than they would have been if formed by gravitational attraction alone, for the repulsive matter in the voids would increase the compaction by pushing in on the clumps of attractive matter from many directions with a nonkinetic, positive pressure *produced by* repulsive gravity, a pressure not to be confused with the negative pseudo-pressure conjectured in the confines of Einstein's assumption to be a *producer of* repulsive gravity.

VI. SUMMARY

Let us now summarize the essential points of the developments detailed above.

- First, analysis of Einstein's argument for the proposition that energy is a source of gravity reveals a gap in the logic, thereby reducing the proposition from a conclusion to an assumption.
- Second, denying that assumption prompts construction of a variational principle that is the most straightforward extension to the general relativity setting of the variational principle that yields the Poisson equation for the newtonian gravitational potential.
- Third, addition of a cosmological constant term to this variational principle shows the cosmological constant to be a negative active gravitational mass density in disguise.
- Fourth, inclusion of a scalar field in the variational principle along with positive and negative mass densities yields field equations essentially different from those of Einstein.
- Fifth, these field equations have cosmological solutions that exhibit acceleration, owed to the negative mass density, coasting, and inflation, owed to the scalar field and the nonstandard polarity of its coupling to the space-time geometry, a coupling polarity consistent with denial of the assumption that energy is a source of gravity.
- Sixth, owing also to the nonstandard polarity of the scalar field coupling, these solutions have no singularity, thus no 'big bang', only a 'big bounce' off a state of maximum compression.
- Seventh, the same field equations, with a time-independent, spatially varying scalar field, have long-known, vacuum, drainhole solutions that, with modifications, model particles capable of serving both as the dark matter holding galaxies and galactic clusters together and as the cosmological-constant 'dark energy' that, in its undisguised form, is seen to be a repulsive gravitational mass density driving the accelerating expansion of the universe.
- Eighth, the repulsive and the attractive sides of these drainholes would likely segregate themselves into the great material voids of the universe and the dark matter clumped around the walls, filaments, and nodes that border the voids.

One can with some confidence assert, on the basis of these eight points, that cosmic acceleration, inflation, dark matter, and dark 'energy', not to mention coasting, voids, walls, filaments, and nodes, have been found wrapped in one neat package, namely, the variational principle $\delta\int[\boldsymbol{R} - \frac{8\pi\kappa}{c^2}(\mu+\bar{\mu}) + 2\,\phi^{\cdot\gamma}\phi_{.\gamma}]\,|g|^{\frac{1}{2}}d^4x = 0$ and the field equations it implies.

APPENDIX A

The Mathematica program exhibited here with the outputs of a sample run takes as inputs $H(t_0)$, $H_{\max}$, and $Q(t_0)$, where t_0 is the present epoch, solves Eqs. (18), (19), and (32) for A, B, and $R(t_0)$, computes $R_{\min}$, $R_{H_{\max}}$, $R_{Q_{\min}}$, $Q_{\min}$, $R_{H_{\max}}/R_{\min}$, $R_{Q_{\min}}/R_{\min}$, and $R(t_0)/R_{\min}$, then integrates Eq. (32) for the normalized scale factor $S \coloneqq \dot{R}/R$ from 0 seconds to targettime seconds (user specified), subject to the initial conditions $S(0) = 1$ and $\dot{S}(0) = 0$ at the bounce. The inputs $H(t_0)$, $H_{\max}$, and $Q(t_0)$ are set in the file data.m as H0, Hmax, and Q0. The targettime is set in the file IterateS.m.

At http://euclid.colorado.edu/~ellis/ (the author's home page) one can link to and copy the files data.m, solveABR0.m, ProcEqS.m, and IterateS.m, along with a Mathematica notebook, SampleRun.nb, that runs the program and also produces the graph in Fig. 4. Also available there is a more elaborate, interactive Mathematica notebook, CosmicEvolution.nb, and associated files nbdata.m, nbsolveABR0.m, nbProcEqS.m, and nbIterateS.m, with which one can perform all the calculations for the $k = -1$ model with $A > 0$, $A = 0$, or $A < 0$.

```
--------------------------------  Program  ---------------------------------
In[1]:= <<data.m
In[2]:= <<solveABR0.m
In[3]:= <<ProcEqS.m
In[4]:= <<IterateS.m
In[5]:= N[{tRQmin, t100doublings, t0} = t /. \
           {FindRoot[Rsol[t] == N[RQmin,1000], {t, 10^(-10)}, \
                     AccuracyGoal -> 50, PrecisionGoal -> 50, \
                     WorkingPrecision -> 100], \
            FindRoot[Log[2, Ssol[t]] == 100, {t, 0, 10^(-10)}, \
                     AccuracyGoal -> 50, PrecisionGoal -> 50, \
                     WorkingPrecision -> 100], \
            FindRoot[Rsol[t] == N[R0,100], {t, targettime/10}, \
                     AccuracyGoal -> 50, PrecisionGoal -> 50, \
                     WorkingPrecision -> 100]},3]{seconds, seconds, seconds}
In[6]:= Round[{Log[2, 1 + t0], Log[2, Ssol[t0]], Log[2, Ssol[targettime]]}]
In[7]:= N[{Convert[Hsol[t0/100],(Kilo Meter/Second)/(Mega Parsec)], \
           Convert[Hsol[t0/10],(Kilo Meter/Second)/(Mega Parsec)], \
           Convert[Hsol[t0],(Kilo Meter/Second)/(Mega Parsec)], \
           Convert[Hsol[2 t0],(Kilo Meter/Second)/(Mega Parsec)], \
           Convert[Hsol[targettime],(Kilo Meter/Second)/(Mega Parsec)]},5]
In[8]:= {Qsol[t0/100], Qsol[t0/10], Qsol[t0], Qsol[2 t0], Qsol[targettime]}
In[9]:= N[{Q0, Hmax/H0}]     (* = {Row head, Column head} *)
In[10]:= N[Qmin,2]                (* Minimum value attained by the \
                                     acceleration parameter Q. *)
In[11]:= N[tRQmin,2] Second       (* Time at which Q reached its minimum. *)
In[12]:= N[t100doublings,2] Second     (* Time elapsed during the first 100 \
                                          doublings of the scale factor R. *)
In[13]:= N[Convert[t0 Second, Year],3]/ \
                  (10^9 Year) Giga Year    (* Time elapsed from the \
                                              bounce to the present. *)
In[14]:= N[Log[2, Ssol[t0]],4]    (* Number of doublings of the scale factor \
                                     R between the bounce and the present. *)
In[15]:= Play[Sin[2Pi 440 t], {t, 0, 1}]
In[16]:= Exit
-----------------------------  End of program  -----------------------------

------------------------------------------------------------------------------
(***************************  filename: data.m  ***************************)
<<Miscellaneous`PhysicalConstants`
<<Miscellaneous`Units`
$MaxPrecision = Infinity
$MaxExtraPrecision = Infinity
USimplify[x_] := Simplify[x, Assumptions -> {Meter > 0, Centimeter > 0,
                                             Second > 0, Year > 0}]

 (*****  Enter input data in rational number form (no decimal points).  *****)

     H0 = 72 (Kilo Meter/Second)/(Mega Parsec) (* H0 := H(t0); t0 is the    *)
   Hmax = (5 10^60) H0                         (* present epoch in seconds. *)
     Q0 = 1/2                                  (* Q0 := Q(t0); Q0 must be   *)
                                               (* between 0 and 1.          *)

 (*****************************************************************************)
```

```
      k = -1/Centimeter^2
      c = Convert[SpeedOfLight, Centimeter/Second]
  H0sec = Convert[H0, 1/Second]
Hmaxsec = Convert[Hmax, 1/Second]
   H0cm = H0sec/c
 Hmaxcm = Hmaxsec/c

Print[StringForm[" "]]
Print[StringForm["k = ``,  c = ``,  c^2 k = ``",
                 N[k]  ,  N[c]  ,  N[c^2 k]    ]]
Print[StringForm[" "]]
Print[StringForm["H0 = `` = ``,  H0/c = ``",
                 H0, N[H0sec], N[H0cm]  ]]
Print[StringForm[" "]]
Print[StringForm["Hmax = `` = ``,  Hmax/c = ``",
                 N[Hmax], N[Hmaxsec], N[Hmaxcm] ]]
Print[StringForm[" "]]
Print[StringForm["Q0 = ``,  Hmax/H0 = ``",
                 N[Q0]  ,  N[Hmax/H0] ]]
Print[StringForm["Memory in use:  ``",
                 N[MemoryInUse[]/2^20,5] megabytes]]
(*****************************  End of file data.m  *****************************)

-------------------------------------------------------------------------------
(**************************  filename: solveABR0.m  **************************)
(*****************************************************************************)
(*                                                                           *)
(*  This Mathematica subprogram take the inputs from data.m, computes in     *)
(*  terms of the input parameters H0, Q0, and Hmax the parameters A, B,      *)
(*  and R0 that satisfy the equations                                        *)
(*                                                                           *)
(*                          2                                                *)
(*                        H0    A   3 k    B                               *)
(*                        --- = - - --- - --- ,                             *)
(*                         2    3     2     6                              *)
(*                        c         R0    R0                               *)
(*                                                                           *)
(*                          2             3/2                              *)
(*                      Hmax    A   2 (-k)                                   *)
(*                      ----- = - + --------- ,                              *)
(*                        2     3       1/2                                 *)
(*                       c           3 B                                     *)
(*                                                                           *)
(*                                    2      4                               *)
(*                                   c  (k R0  + B)                          *)
(*  and                    Q0 = 1 + -------------- ,                        *)
(*                                       2   6                               *)
(*                                     H0  R0                                *)
(*                                                                           *)
(*  and computes from them other parameters of interest.                     *)
(*                                                                           *)
(*****************************************************************************)

(*
t0 := present epoch in seconds
```

```
H0 := H(t0)
Q0 := Q(t0)
R0 := R(t0)

 X := H0/c
 Y := Hmax/c
 Z := Q0

k0 := k/R0^2                    (* k0 = curvature of space at present epoch. *)
B0 := B/R0^6

X^2 = H0^2/c^2
    = A/3 - k/R0^2 - B/(3 R0^6)
    = A/3 - k0 - B0/3
Y^2 = Hmax^2/c^2
    = A/3 + 2 (-k)^(3/2)/(3 Sqrt[B])
    = A/3 + 2 (-k0)^(3/2)/(3 Sqrt[B0])
  Z = Q0
    = 1 + k/((H0^2/c^2) R0^2) + B/((H0^2/c^2) R0^6)
    = 1 + k0/X^2 + B0/X^2
*)

Clear[X, Y, Z, A, B, k0, R0, B0]
X = H0sec/c; Y = Hmaxsec/c; Z = Q0;
R0 = Sqrt[k/k0]
B0 = X^2 (Z - 1) - k0
A = 3 X^2 + 3 k0 + B0
B = B0 R0^6

(*  The formula below for k0 was obtained by solving the X^2, Y^2, and Z     *)
(*  equations in an ancillary Mathematica session.                           *)

k0 = USimplify[(3 (X^2 (Z + 2) - 3 Y^2)(X^2 (Z - 2) + Y^2) +
               Sqrt[3] Sqrt[(X^2 (Z + 2) - 3 Y^2)^3 (X^2 (3 Z - 2) - Y^2)])/
               (24 (X^2 - Y^2))]

Print[StringForm[" "]]
Print[StringForm["curvature of space at present epoch = k0 = ``",
                                                        N[N[k0,1000]] ]]
RHmax = (B/(-k))^(1/4)
Q[R_] := 1 + c^2 (k R^4 + B)/(H[R]^2 R^6)
H[R_] := c Sqrt[(A R^6 - 3 k R^4 - B)/(3 R^6)]

Print[StringForm[" "]]
Print[StringForm["A = ``,  B = ``,  R0 = ``",
                 N[N[A,1000]], N[N[B,1000]], N[N[R0,1000]] ]]
Print[StringForm[" "]]
Print[StringForm["c^2 A = `` = ``,  c^2 B = ``",
                 N[N[c^2 A,1000]], N[N[c^2 A (31557600 Second/Year)^2,1000]],
                                   N[N[c^2 B,1000]] ]]

(*  The formula below for Rminsqr was obtained by solving the equation       *)
(*                                                                           *)
(*            (1/c^2) H^2(R) = (A R^6 - 3 k R^4 - B)/(3 R^6) = 0             *)
(*                                                                           *)
(*  for R^2 in an ancillary Mathematica session.                             *)
```

```
Rminsqr = If[USimplify[(A^2 B + 4 k^3) Centimeter^6] >= 0,
             USimplify[(k/A) (1 + 2^(1/3) k/
                       (A^2 B + 2 k^3 + Sqrt[A^2 B (A^2 B + 4 k^3)])^(1/3) +
                       (A^2 B + 2 k^3 + Sqrt[A^2 B (A^2 B + 4 k^3)])^(1/3)/
                       (2^(1/3) k))],
             (k/A)(1 - 2 Cos[theta/3])]
theta = USimplify[Pi/2 - ArcTan[(A^2 B + 2 k^3)/Sqrt[-A^2 B (A^2 B + 4 k^3)]]]
Rmin = Sqrt[Rminsqr]

Print[StringForm[" "]]
Print[StringForm["Rmin = ``,  RHmax = ``",
                 N[N[Rmin,1000]], N[N[RHmax,1000]] ]]

(*  The formula below for RQminsqr was obtained by solving the equation      *)
(*                                                                           *)
(*       dQ/dR = -2 c^4 (A k R^6 + 3 A B R^2 - 4 B k)/(R^6 H^4(R)) = 0       *)
(*                                                                           *)
(*  for R^2 in an ancillary Mathematica session.                             *)

RQminsqr = USimplify[(B/A)^(1/3)((2 + Sqrt[4 + A^2 B/k^3])^(1/3) +
                                 (2 - Sqrt[4 + A^2 B/k^3])^(1/3))]
RQmin = Sqrt[RQminsqr]; Qmin = Q[RQmin]

Print[StringForm[" "]]
Print[StringForm["RQmin = ``,  Qmin = ``",
                 N[N[RQmin,1000]], N[N[Qmin,1000]] ]]
Print[StringForm[" "]]
Print[StringForm["RHmax/Rmin = ``,  RQmin/Rmin = ``,  R0/Rmin = ``",
                 N[RHmax/Rmin,6], N[RQmin/Rmin,6], N[R0/Rmin,6] ]]
Print[StringForm[" "]]
Print[StringForm["Memory in use:  ``",
                 N[MemoryInUse[]/2^20,5] megabytes]]
(************************  End of file solveABR0.m  ************************)

-------------------------------------------------------------------------------
(*********************  filename: ProcEqS.m (S := R/Rmin)  *********************)
USimplify[x_] := Simplify[x, Assumptions -> {Meter > 0, Centimeter > 0,
                                             Second > 0, Year > 0}]
T1[t_] := USimplify[c^2 A/3 Second^2] S[t]
T2[t_] := (N[USimplify[2 c^2 B Second^2],1000]/N[(3 Rmin^6),1000])/S[t]^5

state = First[NDSolve`ProcessEquations[
              {Sdot'[t] == T1[t] + T2[t],
                  S'[t] == Sdot[t],
                   S[0] == 1, Sdot[0] == 0},
              {S, Sdot}, t,
              AccuracyGoal -> 50, PrecisionGoal -> 50,
              WorkingPrecision -> 100, MaxSteps -> Infinity]]

Print[StringForm[" "]]
Print[StringForm["Memory in use:  ``",
                 N[MemoryInUse[]/2^20,5] megabytes]]
(*************************  End of file ProcEqS.m  *************************)
```

```
--------------------------------------------------------------------------------
(******************  filename: IterateS.m (S := R/Rmin)  *******************)
<<DifferentialEquations`InterpolatingFunctionAnatomy`

targettime = targettimesec = 10^19
targettimeyr = targettimesec/(60*60*24*365)

Print[StringForm[" "]]
Print[StringForm["targettime in seconds = ``;  targettime in years = ``",
                 N[N[targettimesec,1000]]  ,  N[N[targettimeyr,1000]]   ]]

NDSolve`Iterate[state, targettime]

sol = NDSolve`ProcessSolutions[state]

        SSol = S /. sol
      SdotSol = Sdot /. sol
    Ssol[t_] := S[t] /. sol
    Rsol[t_] := N[Rmin Ssol[t],1000]
 Sdotsol[t_] := Sdot[t] /. sol
   T1sol[t_] := N[N[USimplify[c^2 A/3 Second^2],1000]] Ssol[t]
   T2sol[t_] := (N[USimplify[2 c^2 B Second^2],1000]/
                            N[(3 Rmin^6),1000])/Ssol[t]^5
Sddotsol[t_] := T1sol[t] + T2sol[t]
 Hsqrsol[t_] := USimplify[c^2 (N[A/3,1000] - N[k/Rsol[t]^2,1000]
                                  - N[B/(3 Rsol[t]^6),1000])]
    Hsol[t_] := USimplify[Sqrt[Hsqrsol[t]]]
    Qsol[t_] := (Sddotsol[t]/Ssol[t])/(Sdotsol[t]/Ssol[t])^2

{lowtime, hightime} = InterpolatingFunctionDomain[First[S /. sol]][[1,1]]

Print[StringForm[" "]]
Print[StringForm["lowtime = ``,  hightime = ``",
                 N[lowtime]  ,  N[hightime]    ]]
Print[StringForm[" "]]
Print[StringForm["Ssol[targettime] = ``,  Rsol[targettime] = ``",
                 N[Ssol[targettime]]  ,  N[Rsol[targettime]]    ]]
Print[StringForm[" "]]
Print[StringForm["Hsol[targettime] = `` = ``",
                 N[Hsol[targettime]],
                 N[Convert[Hsol[targettime],
                           (Kilo Meter)/(Mega Parsec Second)]] ]]
Print[StringForm[" "]]
Print[StringForm["Memory in use:  ``",
                 N[MemoryInUse[]/2^20,5] megabytes]]
(*************************  End of file IterateS.m  **************************)

--------------------------------------------------------------------------------
------------------------  Sample run of the program  --------------------------
In[1]:= <<data.m
                                10                                    20
        -1.           2.99792 10   Centimeter           -8.98755 10
k = -----------,  c = -----------------------,  c^2 k = -------------
              2               Second                                2
    Centimeter                                           Second
```

```
                                    -18                   -29
       72 Kilo Meter      2.33334 10             7.7832 10
H0 = ------------------ = -------------,  H0/c = ------------
     Mega Parsec Second      Second               Centimeter

             62                          43                      32
       3.6 10   Kilo Meter   1.16667 10             3.8916 10
Hmax = ------------------- = ------------,  Hmax/c = -----------
       Mega Parsec Second       Second               Centimeter
                           60
Q0 = 0.5,  Hmax/H0 = 5. 10

Memory in use:  3.1284 megabytes

In[2]:= <<solveABR0.m
                                                 -57
                                          -3.02891 10
curvature of space at present epoch = k0 = --------------
                                                 2
                                           Centimeter
              -57                 -131
    9.08673 10          1.93778 10                      28
A = -------------,  B = --------------,  R0 = 1.81701 10
               2                   2
     Centimeter          Centimeter

                  -36             -21                     -110
        8.16674 10      8.13311 10              1.74159 10
c^2 A = ------------- = -------------,  c^2 B = --------------
                 2              2                       2
           Second           Year                  Second

                 -33                    -33
Rmin = 1.59421 10   ,  RHmax = 2.0981 10

                  -13                    -82
RQmin = 4.52022 10   ,  Qmin = 9.28318 10
                                                20                       61
RHmax/Rmin = 1.31607,  RQmin/Rmin = 2.83540 10  ,  R0/Rmin = 1.13975 10

Memory in use:  4.4273 megabytes

In[3]:= <<ProcEqS.m

Memory in use:  4.4803 megabytes

In[4]:= <<IterateS.m
                             19                                    11
targettime in seconds = 1. 10  ;  targettime in years = 3.17098 10

                               19
lowtime = 0.,  hightime = 1. 10

                             67                                  35
Ssol[targettime] = 8.34272 10  ,  Rsol[targettime] = 1.33001 10
```

```
                           -18
                  1.64992 10      50.9117 Kilo Meter
Hsol[targettime] = ------------ = ------------------
                      Second       Mega Parsec Second

Memory in use:  189.89 megabytes

In[5]:= N[{tRQmin, t100doublings, t0} = t /. \
           {FindRoot[Rsol[t] == N[RQmin,1000], {t, 10^(-10)}, \
                     AccuracyGoal -> 50, PrecisionGoal -> 50, \
                     WorkingPrecision -> 100], \
            FindRoot[Log[2, Ssol[t]] == 100, {t, 0, 10^(-10)}, \
                     AccuracyGoal -> 50, PrecisionGoal -> 50, \
                     WorkingPrecision -> 100], \
            FindRoot[Rsol[t] == N[R0,100], {t, targettime/10}, \
                     AccuracyGoal -> 50, PrecisionGoal -> 50, \
                     WorkingPrecision -> 100]},3]{seconds, seconds, seconds}

               -23                 -14                 17
Out[5]= {1.51 10    seconds, 6.74 10    seconds, 5.34 10   seconds}

In[6]:= Round[{Log[2, 1 + t0], Log[2, Ssol[t0]], Log[2, Ssol[targettime]]}]

Out[6]= {59, 203, 226}

In[7]:= N[{Convert[Hsol[t0/100],(Kilo Meter/Second)/(Mega Parsec)], \
           Convert[Hsol[t0/10],(Kilo Meter/Second)/(Mega Parsec)], \
           Convert[Hsol[t0],(Kilo Meter/Second)/(Mega Parsec)], \
           Convert[Hsol[2 t0],(Kilo Meter/Second)/(Mega Parsec)], \
           Convert[Hsol[targettime],(Kilo Meter/Second)/(Mega Parsec)]},5]

         5776.6 Kilo Meter   579.14 Kilo Meter   72.000 Kilo Meter
Out[7]= {------------------, ------------------, ------------------,
         Mega Parsec Second  Mega Parsec Second  Mega Parsec Second

     54.000 Kilo Meter   50.912 Kilo Meter
>    ------------------, ------------------}
     Mega Parsec Second  Mega Parsec Second

In[8]:= {Qsol[t0/100], Qsol[t0/10], Qsol[t0], Qsol[2 t0], Qsol[targettime]}

Out[8]= {0.0000776779, 0.00772814, 0.5, 0.888889, 1.}

In[9]:= N[{Q0, Hmax/H0}]     (* = {Row head, Column head} *)

                   60
Out[9]= {0.5, 5. 10  }

In[10]:= N[Qmin,2]                (* Minimum value attained by the \
                                     acceleration parameter Q. *)
              -82
Out[10]= 9.3 10

In[11]:= N[tRQmin,2] Second       (* Time at which Q reached its minimum. *)
```

```
                -23
Out[11]= 1.5 10    Second

In[12]:= N[t100doublings,2] Second     (* Time elapsed during the first 100 \
                                          doublings of the scale factor R. *)
                -14
Out[12]= 6.7 10    Second

In[13]:= N[Convert[t0 Second, Year],3]/ \
                  (10^9 Year) Giga Year    (* Time elapsed from the \
                                              bounce to the present. *)
Out[13]= 16.9 Giga Year

In[14]:= N[Log[2, Ssol[t0]],4]    (* Number of doublings of the scale factor \
                                     R between the bounce and the present. *)
Out[14]= 202.8

In[15]:= Play[Sin[2Pi 440 t], {t, 0, 1}]

Out[15]= -Sound-

In[16]:= Exit
---------------------  End of sample run of the program  ----------------------
--------------------------------------------------------------------------------
```

APPENDIX B

TABLE I: This table presents results of running the Mathematica program of Appendix A for thirty-five choices of the inputs $H_{\max}$ and $Q(t_0)$, all with $H(t_0) = 72$ (km/sec)/Mpc. In each cell the output entries are (a) the minimum value reached by Q, (b) the time at which that minimum value was reached, (c) the time at which the scale factor R attained the 100th doubling of its minimum value at the bounce, (d) the time t_0 of the present epoch, and (e) the number of doublings of R attained at the present epoch. All times are times elapsed since the bounce. The results in the center cell are from the sample run of Appendix A, for which $H_{\max} = 5 \times 10^{60} H(t_0)$ and $Q(t_0) = 1/2$, and which produced the graph of Fig. 4. Every run produces a graph much like Fig. 4 in its overall shape. The results in the upper righthand corner cell, for which $H_{\max} = 1 \times 10^{80} H(t_0)$ and $Q(t_0) = 0.001$, provide perhaps the best match to widely accepted inferences drawn from recent observational data.

$H_{\max}/H(t_0) \rightarrow$ $Q(t_0) \downarrow$	1.0×10^{50}	1.0×10^{55}	5.0×10^{60}	1.0×10^{75}	1.0×10^{80}
0.001	(a) 2.7×10^{-69} (b) 5.8×10^{-16} s (c) 3.4×10^{-3} s (d) 13.6 Gyr (e) 166.8	5.8×10^{-76} 2.7×10^{-19} s 3.4×10^{-8} s 13.6 Gyr 183.4	1.5×10^{-83} 4.2×10^{-23} s 6.7×10^{-14} s 13.6 Gyr 202.3	1.3×10^{-102} 1.2×10^{-32} s 3.4×10^{-28} s 13.6 Gyr 249.8	2.7×10^{-109} 5.8×10^{-36} s 3.4×10^{-33} s 13.6 Gyr 266.4
0.01	(a) 1.3×10^{-68} (b) 3.9×10^{-16} s (c) 3.4×10^{-3} s (d) 13.6 Gyr (e) 166.8	2.7×10^{-75} 1.8×10^{-19} s 3.4×10^{-8} s 13.6 Gyr 183.4	6.8×10^{-83} 2.9×10^{-23} s 6.7×10^{-14} s 13.6 Gyr 202.3	5.8×10^{-102} 8.5×10^{-33} s 3.4×10^{-28} s 13.6 Gyr 249.8	1.3×10^{-108} 3.9×10^{-36} s 3.4×10^{-33} s 13.6 Gyr 266.5
0.1	(a) 5.8×10^{-68} (b) 2.7×10^{-16} s (c) 3.4×10^{-3} s (d) 14.1 Gyr (e) 166.9	1.3×10^{-74} 1.2×10^{-19} s 3.4×10^{-8} s 14.1 Gyr 183.5	3.2×10^{-82} 2.0×10^{-23} s 6.7×10^{-14} s 14.1 Gyr 202.4	2.7×10^{-101} 5.8×10^{-33} s 3.4×10^{-28} s 14.1 Gyr 249.9	5.8×10^{-108} 2.7×10^{-36} s 3.4×10^{-33} s 14.1 Gyr 266.5
0.5	(a) 1.7×10^{-67} (b) 2.0×10^{-16} s (c) 3.4×10^{-3} s (d) 16.9 Gyr (e) 167.3	3.7×10^{-74} 9.5×10^{-20} s 3.4×10^{-8} s 16.9 Gyr 183.9	9.3×10^{-82} 1.5×10^{-23} s 6.7×10^{-14} s 16.9 Gyr 202.8	7.9×10^{-101} 4.4×10^{-33} 3.4×10^{-28} 16.9 Gyr 250.3	1.7×10^{-107} 2.0×10^{-36} s 3.4×10^{-33} s 16.9 Gyr 266.9
0.9	(a) 2.5×10^{-67} (b) 1.9×10^{-16} s (c) 3.4×10^{-3} s (d) 26.0 Gyr (e) 168.4	5.5×10^{-74} 8.6×10^{-20} s 3.4×10^{-8} s 26.0 Gyr 185.1	1.4×10^{-81} 1.4×10^{-23} s 6.7×10^{-14} s 26.0 Gyr 204.0	1.2×10^{-100} 4.0×10^{-33} s 3.4×10^{-28} s 26.0 Gyr 251.5	2.5×10^{-107} 1.9×10^{-36} s 3.4×10^{-33} s 26.0 Gyr 268.1
0.99	(a) 2.7×10^{-67} (b) 1.8×10^{-16} s (c) 3.4×10^{-3} s (d) 40.9 Gyr (e) 170.1	5.8×10^{-74} 8.5×10^{-20} s 3.4×10^{-8} s 40.9 Gyr 186.7	1.5×10^{-81} 1.3×10^{-23} s 6.7×10^{-14} s 40.9 Gyr 205.6	1.3×10^{-100} 3.3×10^{-33} s 3.4×10^{-28} s 40.9 Gyr 253.2	2.7×10^{-107} 1.8×10^{-36} s 3.4×10^{-33} s 40.9 Gyr 269.8
0.999	(a) 2.7×10^{-67} (b) 1.8×10^{-16} s (c) 3.4×10^{-3} s (d) 56.4 Gyr (e) 171.8	5.8×10^{-74} 8.5×10^{-20} s 3.4×10^{-8} s 56.4 Gyr 188.4	1.5×10^{-81} 1.3×10^{-23} s 6.7×10^{-14} s 56.4 Gyr 207.3	1.3×10^{-100} 3.9×10^{-33} s 3.4×10^{-28} s 56.4 Gyr 254.8	2.7×10^{-107} 1.8×10^{-36} s 3.4×10^{-33} s 56.4 Gyr 271.4

[1] A. Einstein, Die Grundlage der allgemeinen Relativitätstheorie, *Ann. der Physik* **49**, translated in *The Principle of Relativity* (Dover, New York, 1952), pp. 109–164.

[2] G. Galilei, **Dialogues Concerning Two New Sciences** (Prometheus Books, Buffalo, N.Y., 1991), pp. 61 *et seq.*; http://galileoandeinstein.physics.virginia.edu/tns_draft/index.html, pp. 61 *et seq.*

[3] A. Einstein, **Relativity, The Special and the General Theory: A Popular Exposition** (Methuen, London, 1916), (Bonanza Books, New York, 1961), pp. 66 *et seq.*; also available as an eBook (Routledge, London, New York, 2002).

[4] D. F. Bartlett and D. Van Buren, Equivalence of active and passive gravitational mass using the moon, *Phys. Rev. Lett.* **57** (1986), 21–24.

[5] L. B. Kreuzer, Experimental measurement of the equivalence of active and passive gravitational mass, *Phys. Rev.* **169** (1968), 1007–1012.

[6] C. S. Unnikrishnan and G. T. Gillies, Do leptons generate gravity? First laboratory constraints obtained from some G experiments and possibility of a new decisive constraint, *Phys. Lett. A* **288** (2001), 161–166.

[7] D. Hilbert, Die Grundlagen der Physik, *Konigl. Gesellschaft d. Wiss. Göttingen, Nachr., Math.-Phys. Kl.*, 395–407; reprised in *Math. Annalen* **92** (1924), 1–32.

[8] A. H. Guth, Time since the beginning, *Astrophysical Ages and Time Scales, Astron. Soc. Pac. conf. ser.*, **245** (2001), 3–17.

[9] H. G. Ellis, Ether flow through a drainhole: a particle model in general relativity, *J. Math. Phys.* **14** (1973), 104–118; Errata: **15** (1974), 520.

[10] K. A. Bronnikov, Scalar-tensor theory and scalar charge, *Acta Phys. Pol.* **B4** (1973), 251–266.

[11] G. Clément, The Ellis Geometry (Letter to the editor), *Am. J. Phys.* **57** (1989), 967.

[12] M. S. Morris and K. S. Thorne, Wormholes in spacetime and their use for interstellar travel: a tool for teaching general relativity, *Am. J. Phys.* **56** (1988), 395–412.

[13] L. Chetouani and G. Clément, Geometrical-optics in the Ellis geometry, *Gen. Relativ. Gravit.* **16** (1984), 111–119.

[14] G. Clément, Scattering of Klein-Gordon and Maxwell waves by an Ellis geometry, *Int. J. Theor. Phys.* **23** (1984), 335–350.

[15] C. Armendáriz-Picón, On a class of stable, traversable Lorentzian wormholes in classical general relativity, *Phys. Rev. D* **65** (2002), 104010-1–10.

[16] T. Matos and D. Nuñez, Rotating scalar field wormhole, *Class. Quantumn Grav.* **23** (2006), 4485–4495.

[17] G Gilmore, M Wilkinson, J Kleyna, A Koch, W Evans, R. F. G. Wyse, E. K. Grebel, Observed properties of dark matter: dynamical studies of dSph galaxies, *Nucl. Phys. B* (in press); arXiv: astro-ph/0608528.

[18] D. Clowe, M. Bradač, A. H. Gonzalez, M. Markevitch, S. W. Randall, C. Jones, and D. Zaritsky, A direct empirical proof of the existence of dark matter, *Astrophys. J. Lett.* **648** (2006), L109–L113.

[19] H. G. Ellis, The evolving, flowless drainhole: A nongravitating-particle model in general relativity theory, *Gen. Relativ. Gravit.* **10** (1979), 105–123.

[20] P. J. E. Peebles, The void phenomenon, *Astrophys. J.* **557** (2001), 495–504.